Diagonal and collinear incommensurate spin structures in underdoped La$_{2-x}$Ba$_x$CuO$_4$

S. R. Dunsiger,[1] Y. Zhao,[1] B. D. Gaulin,[1,2] Y. Qiu,[3,4] P. Bourges,[5] Y. Sidis,[5] J. R. D. Copley,[6] A. Kallin,[1] E. M. Mazurek,[1] and H. A. Dabkowska[1]

[1]*Department of Physics and Astronomy, McMaster University, Hamilton, Ontario, Canada L8S 4M1*
[2]*Canadian Institute for Advanced Research, 180 Dundas Street W., Toronto, Ontario, Canada M5G 1Z8*
[3]*National Institute of Standards and Technology, Gaithersburg, Maryland 20899-6102, USA*
[4]*University of Maryland, College Park, Maryland 20742, USA*
[5]*Laboratoire Léon Brillouin, CEA-Saclay (UMR12 CEA-CNRS), 91191 Gif-sur-Yvette Cedex, France*
[6]*National Institute of Standards and Technology, 100 Bureau Drive, MS 6100, Gaithersburg, Maryland 20899-6100, USA*

We have studied incommensurate spin ordering in single-crystal underdoped La$_{2-x}$Ba$_x$CuO$_4$ with $x \sim 0.08$, 0.05, and 0.025 using neutron-scattering techniques. Static incommensurate magnetic order is observed in the La$_{2-x}$Ba$_x$CuO$_4$ ($x=0.05$ and 0.025) compounds with ordering wave vectors which are rotated by 45° about the commensurate (0.5,0.5,0) position, with respect to that in the superconducting $x=0.08$ material. These spin modulations are one dimensional in the $x=0.05$ and 0.025 samples, with ordering wave vectors lying along the orthorhombic b^* direction. Such a rotation in the orientation of the static spin ordering as a function of increasing Ba doping, from diagonal to collinear, is roughly coincident with the transition from an insulating to a superconducting ground state and is similar to that observed in the related La$_{2-x}$Sr$_x$CuO$_4$ system. This phenomenon is therefore a more generic property of underdoped La-214 cuprates.

PACS number(s): 74.72.Dn, 75.25.+z, 75.30.Fv

Lamellar copper oxides exhibit a wealth of fascinating phenomena which are a sensitive function of doping, evolving from an antiferromagnetic insulating Néel state through a Mott-Hubbard metal-insulator transition into a superconducting phase with increasing hole density.[1] A heterogeneous electronic phase composed of itinerant charges now appears to be a generic feature of the cuprates, although the true nature of the incommensurate spin ordered states is the subject of ongoing debate. In an itinerant picture, the spin dynamics are described in terms of electron-hole pair excitations about an underlying Fermi surface.[2] Alternatively, within the "stripe" picture of doped, two-dimensional Mott insulators, the nonmagnetic holes in these materials organize into quasi-one-dimensional stripes which separate antiferromagnetic insulating antiphase domains.[3] Adjacent antiferromagnetic regions are π out of phase with each other giving rise to a magnetic structure with incommensurate periodicity, where the supercell dimension is twice the hole stripe periodicity.

The static spin structure in the undoped, parent compound La$_2$CuO$_4$ has been determined by neutron scattering to be a simple two sublattice antiferromagnet characterized by a commensurate ordering wave vector of (0.5,0.5,0) in reciprocal-lattice units, or at the (π, π) position within the tetragonal basal plane.[4] On hole doping with Sr^{2+} substituting for La^{3+} in La$_{2-x}$Sr$_x$CuO$_4$, the magnetic scattering moves out to incommensurate wave vectors.[5] Lightly doped La$_{2-x}$Sr$_x$CuO$_4$ displays elastic incommensurate magnetic Bragg peaks which first appear split off from the (0.5,0.5,0) position in diagonal directions relative to a tetragonal unit cell;[6,7] that is at $(0.5 \pm \frac{\delta}{\sqrt{2}}, 0.5 \mp \frac{\delta}{\sqrt{2}}, 0)$ and $(0.5 \pm \frac{\delta}{\sqrt{2}}, 0.5 \pm \frac{\delta}{\sqrt{2}}, 0)$ ordering wave vectors. At higher doping in the underdoped superconducting regime, the Bragg peaks rotate by 45° to lie along directions parallel to or collinear with, the tetragonal axes or Cu-O-Cu bonds, such that elastic magnetic

scattering appears at $(0.5 \pm \delta, 0.5, 0)$ and $(0.5, 0.5 \pm \delta, 0)$.[8,9] For optimal and higher doping the static order disappears, but dynamic incommensurate correlations nevertheless persist.[9,10]

Surprisingly, La$_{2-x}$Ba$_x$CuO$_4$, the original high-temperature superconductor,[11] has been much less extensively studied than its sister compound, La$_{2-x}$Sr$_x$CuO$_4$ due to the difficulty of growing single crystals, which has only been recently achieved.[12] In this Brief Report, we report the observation using neutron diffraction of the transition from a diagonal to a collinear incommensurate spin ordering as an increasing function of doping in La$_{2-x}$Ba$_x$CuO$_4$. Elastic "collinear" incommensurate magnetic Bragg peaks are observed at $T=1.5$ K in superconducting La$_{2-x}$Ba$_x$CuO$_4$ ($x=0.08$). In marked contrast, "diagonal" satellite peaks are observed at low temperature at reciprocal space positions rotated by 45° within the (H,K,0) plane for La$_{2-x}$Ba$_x$CuO$_4$ ($x \sim 0.025$ and 0.05). This is analogous to the behavior observed in the La$_{2-x}$Sr$_x$CuO$_4$ materials and shows that such a rotation of the spin structure is a generic feature of the transition from insulating spin-glass ground state to superconducting ground state in the underdoped La-214 cuprates.

We have grown high quality single crystals of La$_{2-x}$Ba$_x$CuO$_4$ with $x=0.08$, 0.05, and 0.025 using floating zone image furnace techniques with a four-mirror Crystal Systems Inc. optical furnance.[13] Samples of La$_{2-x}$Ba$_x$CuO$_4$ near $x=0.125$ display a sequence of crystal structures on lowering the temperature, evolving progressively from high-temperature tetragonal (HTT) ($I4/mmm$) through midtemperature orthorhombic (MTO) (Bmab) to low-temperature tetragonal (LTT) ($P4_2/ncm$).[14] The HTT to MTO structural phase transition at T_{d1} is a sensitive indication of the precise Ba doping level, from which we have determined the Ba concentration in the $x=0.08$ sample ($T_{d1} \sim 305$ K).[13] It is more difficult to precisely quantify the doping levels in the $x=0.05$ and $x=0.025$ samples, where the crystals remain
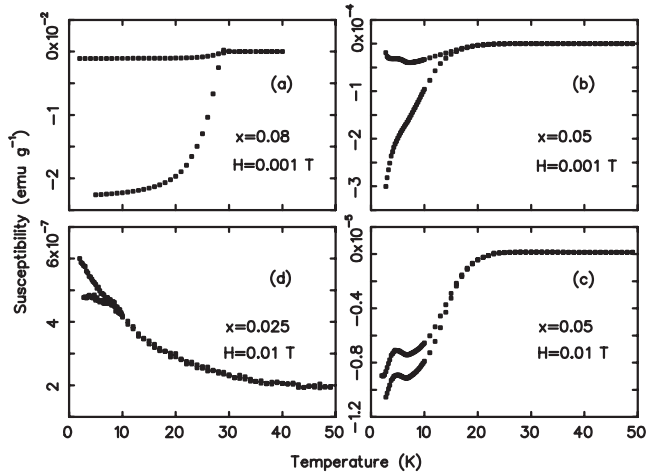
FIG. 1. Zero field cooled and field cooled susceptibilities of $La_{2-x}Ba_xCuO_4$, (a) $x=0.08$, (b) (c) $x=0.05$, and (d) $x=0.025$ single crystals.

orthorhombic at low temperature. As shown in Fig. 1, the diamagnetic superconducting volume fraction in the $x=0.05$ sample is roughly 2 orders of magnitude smaller than the $x=0.08$ sample, placing constraints on the doping level in the nominally $x=0.05$ sample.[12] Similarly, no signature of long-range antiferromagnetic order is observed up to 300 K in the $x=0.025$ sample, setting a lower limit on the doping level of $x>0.02$, by comparison with the suppression of the Néel order in $La_{2-x}Sr_xCuO_4$.

We explore both the spin-glass-like and superconducting regimes of the phase diagram. At the highest Ba concentration, SQUID magnetization measurements indicate a bulk superconducting transition at $T_C=29$ K in the $x=0.08$ sample [see Fig. 1(a)]. In $La_{2-x}Ba_xCuO_4$ ($x=0.05$), a weak superconducting phase transition occurs around 20 K, as evidenced by the weak diamagnetic response [Figs. 1(b) and 1(c)]. Subsequently, history dependent behavior develops below 10 K and a peak in the susceptibility is observed at 5 K, indicating a spin-glass ground state. Finally, at the lowest Ba concentration, dc magnetization measurements indicate the $x=0.025$ sample also undergoes a spin-glass-like transition below ~ 10 K, as shown in Fig. 1(d).

Time-of-flight neutron-scattering measurements were performed using the NG4 disk chopper spectrometer (DCS) at the National Institute for Standards and Technology Center for Neutron Research. The DCS uses choppers to create pulses of monochromatic neutrons whose energy transfers on scattering are determined by their arrival times in the instrument's 913 detectors located at scattering angles from $-30°$ to $140°$. Measurements were performed using 4.8 Å incident neutrons for the $x=0.08$ and 0.05 samples, allowing us to explore the area of reciprocal space around $(0.5,0.5,0)$ with an energy resolution of 118 μeV full width at half maximum (FWHM). Longer wavelength incident neutrons ($\lambda=6.2$ Å with a corresponding energy resolution of 58 μeV FWHM) were used for the $x=0.025$ sample as the anticipated low incommensurability required higher Q resolution. Definitive measurements of the incommensurate spin structure are progressively more difficult at lower doping, as the incommen-
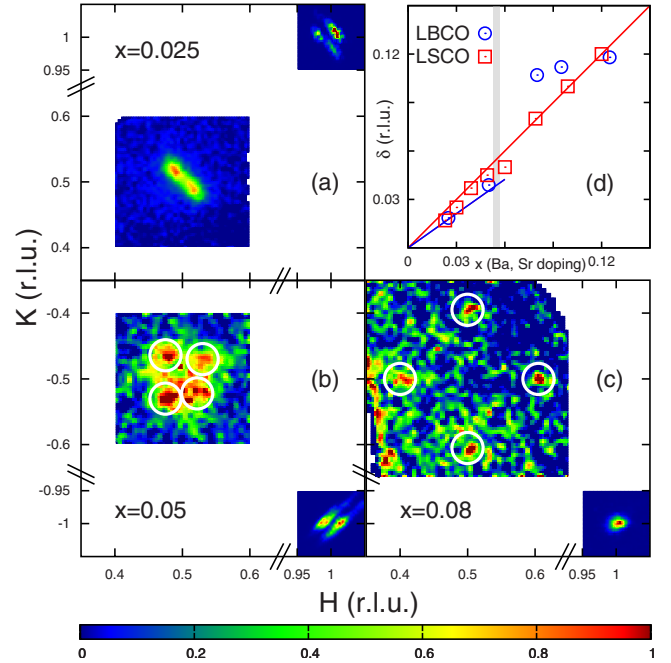

FIG. 2. (Color online) Reciprocal lattice space maps in the $(H,K,0)$ plane, integrating over -0.1 meV $\leq \hbar\omega \leq 0.1$ meV and taken at $T\sim 1.5$ K in $La_{2-x}Ba_xCuO_4$ (a) $x=0.025$, (b) 0.05, and (c) 0.08, respectively. Diagonal magnetic Bragg scattering near $(0.5\pm\frac{\delta}{\sqrt{2}}, 0.5\mp\frac{\delta}{\sqrt{2}}, 0)$ in the $x=0.05$ sample (b) and collinear magnetic Bragg scattering near $(0.5\pm\delta, 0.5, 0)$ and $(0.5, 0.5\pm\delta, 0)$ in the $x=0.08$ sample (c) have been circled for clarity. (d) Incommensurability, δ vs Ba/Sr concentration, x, plotted using the current results and those from the literature, as described in the text. The transition from diagonal to collinear incommensuration in the $La_{2-x}Sr_xCuO_4$ system near $x=0.055$ (Ref. 6) is shown as the shaded vertical line.

surability δ is proportional to the doping level x (Ref. 5). The measurements were carried out using an Institut Laue-Langevin (ILL) orange cryostat with ^{4}He exchange gas to ensure good thermal contact and each sample was aligned with the $(H,K,0)$ plane coincident with the horizontal scattering plane.

Reciprocal space maps at $T\sim 1.5$ K are shown in Fig. 2, where in all cases we have integrated over the elastic scattering between -0.1 meV $\leq \hbar\omega \leq 0.1$ meV. To compare the universal incommensurability in higher doping $La_{2-x}Ba_xCuO_4$ samples and the $La_{2-x}Sr_xCuO_4$ system,[6] we use HTT notation to illustrate the $(H,K,0)$ scattering plane in Fig. 2, where $a=b=3.78$ Å $\simeq a_{ortho}/\sqrt{2}$. Figure 2(a) shows the elastic reciprocal space map from the lightly doped $La_{2-x}Ba_xCuO_4$ ($x=0.025$) compound. These measurements were taken with both 6.2 and 8 Å incident neutrons, in two different Brillouin zones, which gave consistent results [the 6.2 Å data and the zone centered on $(0.5,0.5,0)$ are shown here]. A remarkable, isolated pair of *diagonal* incommensurate magnetic Bragg peaks are evident near $(0.5-\frac{\delta}{\sqrt{2}},0.5+\frac{\delta}{\sqrt{2}},0)$ with an incommensurability $\delta=0.017(1)$, in tetragonal notation. This is clear evidence for a static, one dimensional, diagonal incommensurate spin modulation along b_{ortho}. Nuclear Bragg peaks associated with four MTO

twin domains in the $x=0.025$ sample are visible near $(1,1,0)$ ($\lambda=4.8$ Å). The integrated intensity of the majority twin peak is approximately four times larger than the minority peaks. This accounts for the single pair of incommensurate magnetic Bragg peaks: the magnetic scattering from this $x=0.025$ sample closely resembles that from a detwinned MTO structure with a unique b direction.

The same type of reciprocal space map is shown in Fig. 2(b) for the $x=0.05$ sample, now using $\lambda=4.8$ Å incident neutrons. Two nuclear Bragg peaks are now clear, centered around the tetragonal $(1,-1,0)$ position, associated with two out of four possible twin domains in the sample of La$_{2-x}$Ba$_x$CuO$_4$ ($x=0.05$) at $T=1.5$ K in its MTO phase. The relative intensities of the two $(1,-1,0)$ peaks indicate that the two twin domains have comparable volume fractions. Magnetic Bragg peaks arising from static incommensurate spin order are again observed along the *diagonal* directions that are along each of the b_{ortho} axes. One pair of magnetic Bragg peaks is associated with each twin domain, such that a one-dimensional spin modulation occurs only along the orthorhombic b axis, as clearly illustrated in Fig. 2(b) of Ref 7.

Such diagonal stripes have been predicted theoretically[15] and have also been observed in insulating La$_{2-2x}$Sr$_x$NiO$_4$.[16] The pattern is very similar to that observed in underdoped La$_{2-x}$Sr$_x$CuO$_4$ ($0.02 \leq x \leq 0.055$),[6,7,17] where the diagonal spin modulation is also along the orthorhombic b axis and is considered to be an intrinsic property of the entire insulating spin-glass region, in contrast to the parallel spin modulation observed in the superconducting phase of La$_{2-x}$Sr$_x$CuO$_4$.

By contrast, magnetic Bragg peaks in the La$_{2-x}$Ba$_x$CuO$_4$ $x=0.08$ occur at $(0.5 \pm \delta, 0.5, 0)$ and $(0.5, 0.5 \pm \delta, 0)$ with $\delta=0.107(3)$, as shown in the map of reciprocal space in Fig. 2(c), again measured using $\lambda=4.8$ Å incident neutrons. This indicates static *collinear* incommensurate spin order, with ordering wave vectors parallel to a^*_{tetra}. A single $(1,-1,0)$ structural Bragg peak is evident in Fig. 2(c), indicating the $x=0.08$ sample is in its LTT phase at 1.5 K. Complementary thermal triple axis neutron measurements are described elsewhere.[18]

The magnetic incommensurate ordering wave vectors, δ determined from the data in Figs. 2(a)–2(c) are plotted vs Ba concentration, x, in Fig. 2(d), along with the x dependence of δ in La$_{2-x}$Sr$_x$CuO$_4$.[6] Data from $x=0.095$ and 0.125 samples of La$_{2-x}$Ba$_x$CuO$_4$ (Ref. 18) are also included. While minor differences are evident, the overall δ vs x behavior is very similar in this range of underdoped La$_{2-x}$Ba$_x$CuO$_4$ and La$_{2-x}$Sr$_x$CuO$_4$. The same transition, from diagonal to collinear incommensurate spin ordering is roughly coincident with the transition from an insulating spin-glass ground state to a superconducting ground state near $x_C \sim 0.055$ for both La$_{2-x}$Ba$_x$CuO$_4$ and La$_{2-x}$Sr$_x$CuO$_4$ families, as shown by the vertical line in Fig. 2(d). The complex low-temperature structural phase diagram of La$_{2-x}$Ba$_x$CuO$_4$ with LTT phase and near-complete suppression of superconductivity near $x=0.125$, clearly does not interfere with the rotation of the incommensurate spin ordering as a function of doping.

Complementary cold triple axis neutron-scattering experiments were undertaken on the same La$_{2-x}$Ba$_x$CuO$_4$ ($x=0.05$) single crystal using the 4F1 spectrometer at the Lab-
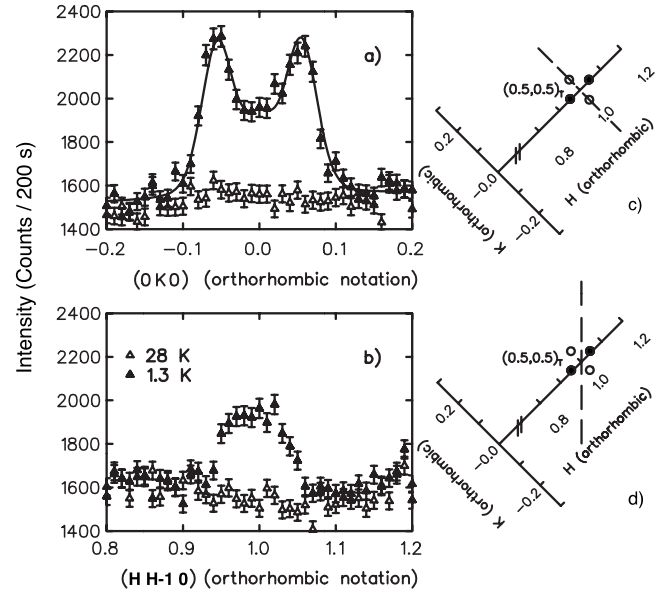

FIG. 3. Static incommensurate magnetic peaks with $\delta=0.039$ in La$_{1.95}$Ba$_{0.05}$CuO$_4$ at $T=1.5$ K, along (a) the orthorhombic b^* $(1,K,0)_O$ or "diagonal" direction, (b) the "collinear" direction. The solid line in Fig. 3(a) is discussed in the text. The open circles in (c) and (d) schematically show the positions of the four diagonal, incommensurate peaks.

oratoire Leon Brillouin, France. The (002) reflection of pyrolytic graphite was used for both monochromator and flat analyzer ($E_i=E_f=5$ meV). We employed open-60′-60′-open collimation along the beam path from source through sample to detector, yielding an energy resolution at $\hbar\omega=0$ of 105 μeV. Cooled Be filters were placed in both the incident and scattered beams to remove contamination from higher order neutrons. The spectrometer was aligned to concentrate on a single twin domain. Representative elastic scans along the orthorhombic and tetragonal b^* axes are shown in Figs. 3(a) and 3(b), respectively, using an orthorhombic coordinate system ($a_{\text{ortho}}=5.3380$ Å, $b_{\text{ortho}}=5.4125$ Å). Well resolved elastic magnetic peaks at an incommensurability $\delta =0.0389(6)$ rlu in tetragonal notation are clearly visible in Fig. 3(a), corresponding to the static spin modulation along the b^* direction. By contrast, the intensity centered on the commensurate position in Figs. 3(b) is due to the tails of the incommensurate peaks coming from the b^* modulation. There is no evidence of any coexistence of diagonal and collinear spin ordering.

Quantitatively, the data in Fig. 3(a) have been analyzed using a resolution convolution of four, one-dimensional Lorentzian functions

$$S(K) = \frac{A}{\pi} \sum_{n=1}^{4} \frac{\kappa}{(K-K_{\delta,n})^2 + \kappa^2} \qquad (1)$$

to extract values for the incommensurate wave vector δ and inverse correlation length κ. $K_{\delta,n}$ represents the four incommensurate wave vectors at $(1, \pm\sqrt{2}\delta, 0)_O$ and $(0.987 \pm \sqrt{2}\delta \cos\theta, 0.0075 \pm \sqrt{2}\delta \sin\theta, 0)_O$. The latter contribution arises from the wings of the second domain, char-

acterized by a nuclear Bragg peak centered at $(1.974, 0.015, 0)_O$, such that $\tan\theta = 0.015/1.974$. The inverse of the static correlation length in the basal plane is defined as the peak half width at half maximum (HWHM) κ. This functional form assumes that the magnetic scattering consists of rods running along the c^* axis. The magnetic peaks are relatively sharp and practically resolution limited, with a HWHM of 0.0038(10) rlu in tetragonal notation, equivalent to a correlation length of 159(50) Å within the basal plane. This is of a comparable magnitude as that observed in the superconducting state of $La_{2-x}Ba_xCuO_4$ ($x=0.095, 0.08$).[18] However, it should be noted that the values quoted for the related $La_{2-x}Sr_xCuO_4$ $x=0.05$ compound are much shorter,[7,19] between 25–35 Å.

The temperature dependence of the incommensurate magnetic elastic scattering is shown in Fig. 4 for the $x=0.05$ and 0.025 samples, which display the diagonal incommensurate spin structures. Triple axis measurements of the magnetic Bragg intensity at $(1, -0.053, 0)_O$ in the $x=0.05$ sample may be compared with DCS measurements of the intensity integrated between $-0.1 \le \hbar\omega \le 0.1$ meV, as the energy resolution is similar. Figure 4 shows the decrease of the static incommensurate magnetic Bragg intensity in the $x=0.05$ sample on warming to $T=10$ K, consistent with the temperature dependence of the break between the field cooled (FC) and zero field cooled (ZFC) susceptibilities shown in Fig. 1(b). For temperatures beyond 10 K, a continued weak fall off of the intensity with increasing temperature is observed to ~25 K, beyond which no vestiges of the static signal are easily observable. Our data for the temperature dependence of the incommensurate magnetic scattering in the $x=0.025$ sample is less extensive, but qualitatively similar to that of the $x=0.05$ sample, as may be expected due to the similarity in the temperature dependence of their ZFC vs FC susceptibilities and therefore their spin-glass ground states.

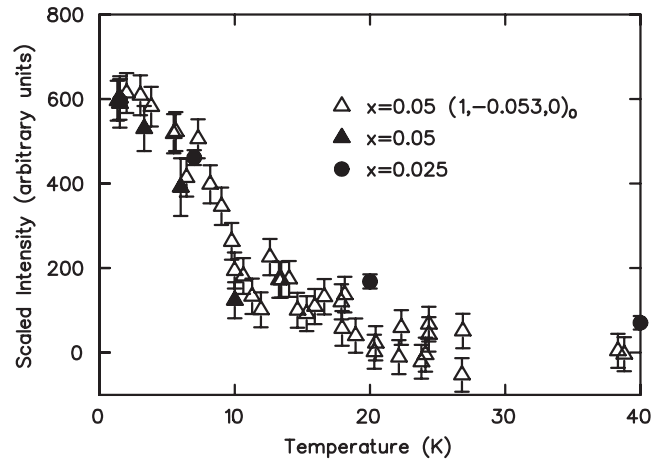In conclusion, we have observed static, *diagonal*, one-

FIG. 4. The temperature dependence of the net elastic incommensurate magnetic scattering in $La_{2-x}Ba_xCuO_4$ ($x=0.05$) measured at $(1, -0.053, 0)_O$ using triple axis (open triangles) and time-of-flight (filled triangles) neutron-diffraction techniques. Integrated intensity between $-0.1 \le \hbar\omega \le 0.1$ meV as a function of temperature in $La_{2-x}Ba_xCuO_4$ ($x=0.025$) measured using the DCS spectrometer (filled circles).

dimensional incommensurate spin ordering in $La_{2-x}Ba_xCuO_4$ with $x=0.05$ and $x=0.025$, evolving into *collinear* incommensurate order in the superconducting $x=0.08$ sample. This result is very similar to the evolution of incommensurate spin order in the well studied underdoped system, $La_{2-x}Sr_xCuO_4$, implying the phenomenon is a generic feature of the underdoped La-214 cuprates.

[1] M. A. Kastner *et al.*, Rev. Mod. Phys. **70**, 897 (1998); J. M. Tranquada, arXiv:cond-mat/0512115 (unpublished); R. J. Birgeneau *et al.*, J. Phys. Soc. Jpn. **75**, 111003 (2006).

[2] N. Bulut *et al.*, Phys. Rev. Lett. **64**, 2723 (1990); N. Bulut and D. J. Scalapino, Phys. Rev. B **53**, 5149 (1996); M. R. Norman, *ibid.* **61**, 14751 (2000).

[3] S. A. Kivelson *et al.*, Rev. Mod. Phys. **75**, 1201 (2003).

[4] D. Vaknin *et al.*, Phys. Rev. Lett. **58**, 2802 (1987).

[5] K. Yamada *et al.*, Phys. Rev. B **57**, 6165 (1998).

[6] M. Matsuda *et al.*, Phys. Rev. B **62**, 9148 (2000).

[7] S. Wakimoto *et al.*, Phys. Rev. B **61**, 3699 (2000).

[8] T. Suzuki *et al.*, Phys. Rev. B **57**, R3229 (1998).

[9] H. Kimura *et al.*, Phys. Rev. B **59**, 6517 (1999).

[10] S. Wakimoto *et al.*, Phys. Rev. Lett. **92**, 217004 (2004).

[11] J. G. Bednorz and K. A. Muller, Z. Phys. B: Condens. Matter **64**,

189 (1986).

[12] T. Adachi, T. Noji, and Y. Koike, Phys. Rev. B **64**, 144524 (2001).

[13] Y. Zhao *et al.*, Phys. Rev. B **76**, 184121 (2007).

[14] J. D. Axe *et al.*, Phys. Rev. Lett. **62**, 2751 (1989).

[15] K. Machida, Physica C **158**, 192 (1989); M. Kato *et al.*, J. Phys. Soc. Jpn. **59**, 1047 (1990); D. Poilblanc and T. M. Rice, Phys. Rev. B **39**, 9749 (1989); H. Schulz, J. Phys. (France) **50**, 2833 (1989); J. Zaanen and O. Gunnarsson, Phys. Rev. B **40**, 7391 (1989).

[16] J. M. Tranquada, D. J. Buttrey, and V. Sachan, Phys. Rev. B **54**, 12318 (1996); H. Yoshizawa *et al.*, *ibid.* **61**, R854 (2000).

[17] S. Wakimoto *et al.*, Phys. Rev. B **60**, R769 (1999).

[18] S. R. Dunsiger *et al.*, Phys. Rev. B **77**, 224410 (2008).

[19] W. Bao *et al.*, Phys. Rev. B **76**, 180406(R) (2007).